

**INTERNATIONAL JOURNAL OF ENGINEERING SCIENCES & RESEARCH  
TECHNOLOGY**
**ANALYSIS OF AXIAL RIGIDITY IN BEARINGS: SPINDLES FROM HIGH  
ROTATION SPEED TECHNOLOGICAL SYSTEMS**
**Popescu Daniel<sup>1\*</sup>, Popescu Roxana-Cristina<sup>2,3</sup>**
<sup>1</sup>Autovehicles Department, Faculty of Mechanics, University of Craiova, Craiova, Romania,

<sup>2</sup>Department of Life and Environmental Sciences, "HoriaHulubei" National Institute of Physics and Nuclear Engineering, Magurele, Bucharest, Romania;

<sup>3</sup>Department of Science and Engineering of Oxide Materials and Nanomaterials, Faculty of Applied Chemistry and Materials Science, Politehnica University of Bucharest, Bucharest, Romania;

**ABSTRACT**

This paper presents a mathematical model for the variation of the axial rigidity of the main shaft in a CNC machine tool. It analyzes the main parameters on which the axial rigidity of the shaft depend and the way they influence the stability of functioning.

**KEYWORDS:** Principal shaft; axial rigidity; parameters; stability.

**INTRODUCTION**

The modern technological working conditions impose a series of structural changes of the main components of a CNC machine tool. One of these is referring to the construction and functioning of the main axle, which must possess an appropriate technological rigidity, in order to obtain dimensional precision and quality of the superior surface. [1]

In this regards, one must know the initial working conditions in stationary mode. Thus, for a fixed shaft, we have [2, 3]:

$$\begin{cases} F_i = F_e = F \\ \alpha_i = \alpha_e = \alpha \end{cases} \quad (1)$$

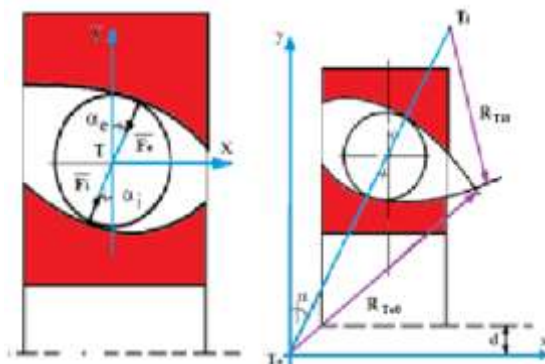


**Figure 1. Technological elements of construction for the idle bearing;**

It is considered a benchmark attached to the exterior ring (fixed) with the origin in the center of the processing arch of the exterior ring,  $T_e$ , and longitudinal axe  $T_{ex}$  and radial axis  $T_{ey}$  (figure 1). [5,6]

We have:

$R_{Teo}$  = the processing range of the exterior ring;

$R_{Tio}$  = the processing range of the interior ring;

The  $T_i$  position of the center of the interior ring from the stated benchmark will have the following coordinates:

$$\begin{cases} X_{T_i} = (R_{Teo} + R_{Tio} - 2r)\sin\alpha \\ Y_{T_i} = (R_{Teo} + R_{Tio} - 2r)\cos\alpha \end{cases} \quad (2)$$

### ANALYSIS OF THE AXIAL RIGIDITY. ESTABLISHING A MATHEMATICAL MODEL FOR THE SIMULATION.

In dynamic mode, the bearing's vibrations will produce relative movements between the interior and the exterior rings. It is considered a movement of the interior ring equal to  $u_1$ .

This is equivalent to a displacement of the interior ring center along  $T_x$  axis with a distance equal to  $u_1$ . The  $T_i$  point will become  $T_i'$  point, which has the following coordinates:

$$\begin{cases} X_{T_i'} = X_{T_i} + u_1 = (R_{Teo} + R_{Tio} - 2r)\sin\alpha + u_1 \\ Y_{T_i'} = Y_{T_i} = (R_{Teo} + R_{Tio} - 2r)\cos\alpha \end{cases} \quad (3)$$

This will produce a displacement of the bead (of its center), its deformation and the runways deformation. We can write:

$$\begin{cases} X_{T_i'} = (R_e - r)\sin\alpha_e + (R_i - r)\sin\alpha_i \\ Y_{T_i'} = (R_e - r)\cos\alpha_e + (R_i - r)\cos\alpha_i \end{cases} \quad (4)$$

By making simplifications, we have:

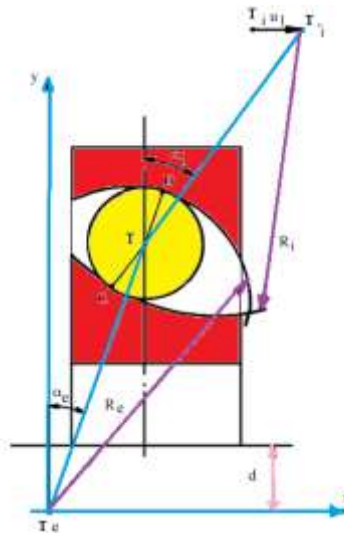


Figure 2. Technological elements of construction for the bearing in case of dynamic stress;

The angle at contact with the rings will become:

$$\begin{cases} \alpha_i = \alpha + \varphi_i \\ \alpha_e = \alpha + \varphi_e \end{cases} \quad (5)$$

The rings deformation will be produced under  $F_e$  and  $F_i$  forces action; these forces are calculated using the following relations, based on the Hertzian contact theory:

$$\begin{cases} F_i = K(R_i - R_i^0) = K \cdot \Delta_i \\ F_e = K(R_e - R_e^0) = K \cdot \Delta_e \end{cases} \quad (6)$$

Where K is a constant which depends on the nature of the materials being in contact, while  $\Delta_i$  and  $\Delta_e$  are the interior, respectively the exterior ring deformations.

In order to analyze the  $k_{11}$  rigidity variation, first of all, we will study the effect of the bearing rotation movement. For this, we must solve the system (5) for an  $u_1=0$  movement. We will have the solutions:

$$\begin{aligned} \varphi_i &= \frac{-2(R_{T_{i0}}-r)tg\alpha}{R_{T_{i0}}-R_{T_{e0}}} & \varphi_e &= \frac{2(R_{T_{e0}}-r)tg\alpha}{R_{T_{i0}}-R_{T_{e0}}} \\ \Delta_i &= -\frac{D\Omega^2\cos\alpha}{2k} & \Delta_e &= \frac{D\Omega^2\cos\alpha}{2k} \end{aligned} \quad (7)$$

$$\text{Where: } D = m_b |R_{T_{e0}} \cdot r \cos\alpha| B^2 \quad (8)$$

The interaction between the bead and the interior ring (respectively the exterior ring) will be:

$$\begin{aligned} F_i &= -\frac{D\Omega^2\cos\alpha}{2} \\ F_e &= \frac{D\Omega^2\cos\alpha}{2} \end{aligned} \quad (9)$$

By introducing a longitudinal displacement  $u_1$ , the bead will continuously deform the rings, with the shifts  $\Delta_i \rightarrow \Delta_i + \Delta_{it}$  and  $\Delta_e \rightarrow \Delta_e + \Delta_{et}$ , while the rotations are  $\varphi_i \rightarrow \varphi_i + \varphi_{it}$  and  $\varphi_e \rightarrow \varphi_e + \varphi_{et}$ .

The system becomes:

$$\begin{cases} \sin\alpha\Delta_i^I + \sin\alpha\Delta_e^I + (R_{T_{i0}} - \Delta_i - r)\cos\alpha\varphi_i^I + (R_{T_{e0}} + \Delta_e - r)\cos\alpha\varphi_e^I = u_1 \\ \cos\alpha\Delta_i^I + \cos\alpha\Delta_e^I - (R_{T_{i0}} - \Delta_i - r)\sin\alpha\varphi_i^I - (R_{T_{e0}} + \Delta_e - r)\sin\alpha\varphi_e^I = 0 \\ k(\sin\alpha + \varphi_i\cos\alpha)\Delta_i^I - k(\sin\alpha + \varphi_e\cos\alpha)\Delta_e^I + F\cos\alpha\varphi_i^I + F\cos\alpha\varphi_e^I = 0 \\ k(\cos\alpha - \varphi_i\sin\alpha)\Delta_i^I - k(\cos\alpha + \varphi_e\sin\alpha)\Delta_e^I - F\sin\alpha\varphi_i^I - F\sin\alpha\varphi_e^I = 0 \end{cases} \quad (10)$$

This is a linear system with the unknown  $\Delta_i$ ,  $\Delta_e$ ,  $\varphi_i$ ,  $\varphi_e$ , where:

$$\Delta_i^I = \frac{m_1}{m}; \quad \Delta_e^I = \frac{m_2}{m}; \quad \varphi_i^I = \frac{m_3}{m}; \quad \varphi_e^I = \frac{m_4}{m}; \quad (11)$$

Also, the axial force, which determines the  $u_1$  displacement, is calculated using eq. (12)

$$\begin{aligned} F_{ax} &= n \cdot k \cdot \Delta_i^I (\sin\alpha + \varphi_i^I \cos\alpha) \\ F_{ax} &= n \cdot k \cdot \frac{d_1}{m} u_1 (\sin\alpha + \varphi_i^I \cos\alpha) + \frac{d_3}{m} u_1 \cos\alpha \end{aligned} \quad (12)$$

And the rigidity

$$\begin{aligned} k_{11} &= \frac{\delta F_{ax}}{\delta u_1} & (13) \\ m_1 &= \begin{bmatrix} u_1 & \sin\alpha & (R_{T_{i0}} + \Delta_i - r)\cos\alpha & (R_{T_{e0}} + \Delta_e - r)\cos\alpha \\ 0 & \cos\alpha & -(R_{T_{i0}} + \Delta_i - r)\sin\alpha & -(R_{T_{e0}} + \Delta_e - r)\sin\alpha \\ 0 & -k(\sin\alpha + \varphi_e \cos\alpha) & F\cos\alpha & F\cos\alpha \\ 0 & -k(\cos\alpha - \varphi_e \sin\alpha) & -F\sin\alpha & -F\sin\alpha \end{bmatrix} \end{aligned}$$

$$\begin{aligned}
 m_2 &= \begin{bmatrix} \sin\alpha & u_1 & (R_{T_{i0}} + \Delta_i - r)\cos\alpha & (R_{T_{e0}} + \Delta_e - r)\cos\alpha \\ \cos\alpha & 0 & -(R_{T_{i0}} + \Delta_i - r)\sin\alpha & -(R_{T_{e0}} + \Delta_e - r)\sin\alpha \\ k(\sin\alpha + \varphi_e \cos\alpha) & 0 & F\cos\alpha & F\cos\alpha \\ k(\cos\alpha - \varphi_e \sin\alpha) & 0 & -F\sin\alpha & -F\sin\alpha \end{bmatrix} \\
 m_3 &= \begin{bmatrix} \sin\alpha & \sin\alpha & u_1 & (R_{T_{e0}} + \Delta_e - r)\cos\alpha \\ \cos\alpha & \cos\alpha & 0 & -(R_{T_{e0}} + \Delta_e - r)\sin\alpha \\ k(\sin\alpha + \varphi_e \cos\alpha) & -k(\sin\alpha + \varphi_e \cos\alpha) & 0 & F\cos\alpha \\ k(\cos\alpha - \varphi_e \sin\alpha) & -k(\cos\alpha - \varphi_e \sin\alpha) & 0 & -F\sin\alpha \end{bmatrix} \\
 m_2 &= \begin{bmatrix} \sin\alpha & \sin\alpha & (R_{T_{i0}} + \Delta_i - r)\cos\alpha & u_1 \\ \cos\alpha & \cos\alpha & -(R_{T_{i0}} + \Delta_i - r)\sin\alpha & 0 \\ k(\sin\alpha + \varphi_e \cos\alpha) & -k(\sin\alpha + \varphi_e \cos\alpha) & F\cos\alpha & 0 \\ k(\cos\alpha - \varphi_e \sin\alpha) & -k(\cos\alpha - \varphi_e \sin\alpha) & -F\sin\alpha & 0 \end{bmatrix}
 \end{aligned} \tag{14}$$

We have:

$$k_{11} = M + 2 \cdot N \cdot u_1$$

$$M = n \cdot k \cdot \frac{d_1}{m} (\sin\alpha + \varphi_i \cos\alpha)$$

$$N = n \cdot k \cdot \frac{d_1 \cdot d_3}{m^2} \cdot \cos\alpha$$

$$k_{11} = \sqrt{M^2 + 4NF_{ax}}$$

$$m = 2kF \left[ R_{T_{i0}} - R_{T_{e0}} - \frac{\Omega^2 \cos\alpha}{k} m_b (R_{T_{e0}} - r \cos\alpha) \frac{(R_e - 2r \cos\alpha - d)^2}{4 \cdot (R_e - r \cos\alpha - d)^2} \right]$$

$$d_1 = kF \sin\alpha \left[ R_{T_{i0}} - R_{T_{e0}} - \frac{\Omega^2 \cos\alpha}{k} m_b (R_{T_{e0}} - r \cos\alpha) \frac{(R_e - 2r \cos\alpha - d)^2}{4 \cdot (R_e - r \cos\alpha - d)^2} \right]$$

$$d_3 = 2kF \cos\alpha + 2k^2 \sin\alpha \cdot \operatorname{tg}\alpha \cdot \left[ R_{T_{i0}} - R_{T_{e0}} - \frac{\Omega^2 \cos\alpha}{k} m_b (R_{T_{e0}} - r \cos\alpha) \frac{(R_e - 2r \cos\alpha - d)^2}{4 \cdot (R_e - r \cos\alpha - d)^2} \right]$$

(15)

By calculating M and N, we have:

$$C_1 = \frac{nk \sin 2\alpha}{F} \cdot [F \cos\alpha + k \sin\alpha \cdot \operatorname{tg}\alpha \cdot (R_{T_{e0}} - r)]$$

$$C_2 = \frac{nk \sin 2\alpha}{F} \cdot \frac{\sin^2 \alpha}{8} \cdot \frac{(R_{T_{e0}} - 2r \cos\alpha)^2}{R_{T_{e0}} - r \cos\alpha}$$

$$C_3 = \frac{m_b \cos\alpha}{4k} \cdot \frac{(R_{T_{e0}} - 2r \cos\alpha)^2}{R_{T_{e0}} - r \cos\alpha}$$

$$k_{11} = \sqrt{M^2 + 4 \cdot \frac{C_1 + C_2 \cdot \Omega^2}{-C_3 \cdot \Omega^2} \cdot F_{ax}}$$

$$A_1 = \frac{4C_1}{C_3}; A_2 = \frac{4C_2}{C_3}$$

$$k_{11} = \sqrt{M^2 - \left(\frac{A_1}{\Omega^2} + A_2\right) \cdot F_{ax}}$$

(16)

For the purpose of establishing a mathematical model for the simulation, it is considered the expression of the dynamic accommodation base load at the rolling contact, which is given by the relation:

$$Q_C = A \cdot \left[ \frac{D_R \cdot D_{C_{i,e}}}{D_w \cdot (D_{C_{i,e}} - D_R)} \right]^{0,41} \cdot \frac{(1 \pm \gamma)^{1,39}}{(1 \pm \gamma)^{1/3}} \cdot \left( \frac{\gamma}{\cos \alpha} \right)^{0,3} \cdot D_w^{1,8} \cdot Z^{-1/3} \quad (17)$$

Where:

$Q_C$  = the basis dynamic load at the rolling contact, for bearings with contact point [N];

A = material constant = 100;

$D_R$  = the double of the curvature radius of the rolling body in the area of contact with the rolling track;

$D_{C_{i,e}}$  = the diameter of the rolling track of the interior/ exterior ring;

$D_w$  = the diameter of the rolling body;

[4, 6, 7, 8]

The simulation was done using MATLAB MathWorks for two typo dimensions of angular contact bearings with beads. The constructive dimensions are given in Table 1 [6].

**Table 1. The constructive dimensions used in the mathematical simulation of the models;**

d (mm)	A	$D_R$ (mm)	$D_{C_i}$ (mm)	$D_w$ (mm)	$\gamma$	$d_m$ (mm)	$\alpha^0$	Y	$Q_C$ (N)	n
40	100	10,16	46	7,94	0,142	53,94	15	1	3298,68	16
25	100	8,62	31	6,75	0,159	41	15	1	2650,97	14

The resulting mathematical models for each case are given by the following expressions:

$$k_{11} = \sqrt{18438 - \left( \frac{7265104,8}{\Omega^2} + 1403,39 \right) F_{ax}}$$

$$k_{11} = \sqrt{7377,766 - \left( \frac{3450741}{\Omega^2} + 1046,956 \right) F_{ax}}$$

(18)

The simulations were done by varying the definition domain of the two parameters  $n_\Omega = 15100 \div 19000$  r/m and  $F_{ax} = 1 \div 10$  (N), corresponding to the results obtained by direct measurements. The results are shown in Figure 3.

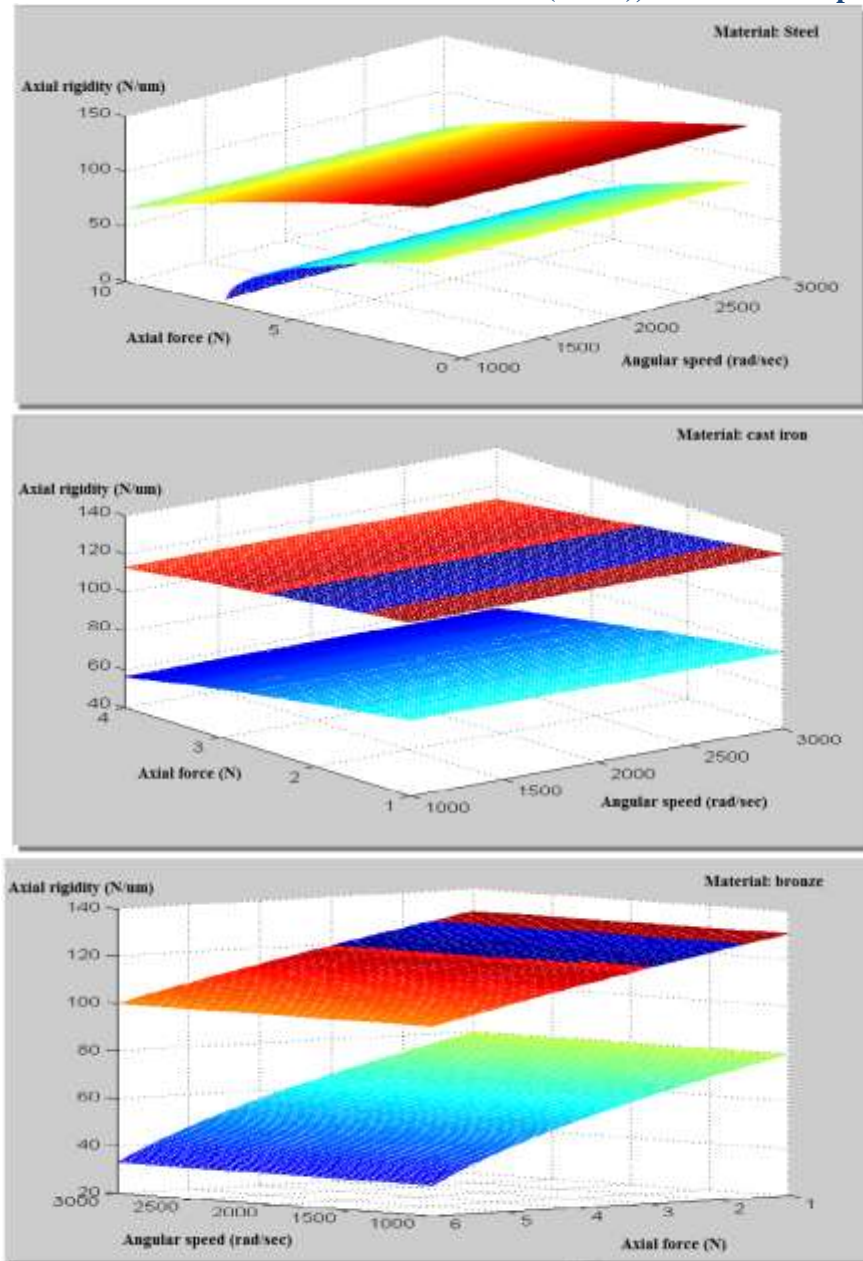


Figure 3- Analysis of bearing axial rigidity in case of the main axis from high rotation speed technological systems;

## CONCLUSION

- 1) The simulations were made for materials for processing like steel, cast iron and bronze;
- 2) The range of the interior grinding spindle angular speed corresponds to the direct experimental measurement ranges:

$$n_{w1} = 15100 \frac{r}{m}; n_{w2} = 17500 \frac{r}{m}; n_{w3} = 19000 \frac{r}{m};$$

- 3) The spindle's final load range corresponds to the direct experimental measurement ranges:



$$F_{ax steel} = 0 \div 10 (N); F_{ax cast iron} = 1 \div 4 (N); F_{ax bronze} = 1 \div 6 (N);$$

- 4) In both cases one can observe a decrease of the axial rigidity with the increase of the final load, with a higher gradient for the real model than the one obtained after the simulation;
- 5) The axial rigidity remains constant or varies very little with the variation of the angular speed of the interior grinding spindle axis.

### REFERENCES

- [1] Folea, M., Lupulescu, N.B., Lancea, C., Economical Impact of Using High Speed Machines, Chisinau: Modern technologies, Quality and Restructuring, VOL. 1, pp. 113-116, 2008
- [2] Ditu, V., The metalscutting basis- Theory and applications. Matrix Rom Publishing, ISBN 978-973-755-444-4, 2008.
- [3] Ispas, C., Simion, F.P., Machine tools vibrations. Theory and applications. Bucharest: Romanian Academy Publishing House, pp. 50-82, 1986
- [4] Landers, R., G., Process Analysis and Control of Machining Operation, Washington University Revue, 2002.
- [5] Popescu, D., Ispas, C., Rectification Processes Dynamics. Craiova: SITECH Publishing, 1999.
- [6] Popescu, D., Theoretical and experimental contribution regarding the machining precision improvement at interior grinding tools., PhD thesis, Politehnica University of Bucharest, 1999.
- [7] Rahnejat H., Gohor R, The Vibrations of Radial Ball Bearings, Mech E, VOL. 199, NO. 3, pp. 181-193, 1985.
- [8] Tudor A., Prodan Gh. Et. al, Mechanical transmissions durability and fiability, Bucharest: E.T, 1988.

### AUTHOR BIBLIOGRAPHY

	<p><b>Daniel Popescu</b> Associate Proffesor at University of Craiova, Faculty of Mechanics; Competence domains: machine tool design, designing machinery for deformation processing, special machinery, industrial logistics, flexible systems for processing, integrated systems for fabrication.</p>
	<p><b>Roxana-Cristina Popescu</b> Engineer at “Horia Hulubei” National Institute of Physics and Nuclear Engineering, Department of Life and Environmental Science; Master Student at Politehnica University of Bucharest, Faculty of Applied Chemistry and Materials Science; Competence domains: nanomaterials, biomaterials, in vitro and in vivo materials testing, stress analysis, computational stress analysis and modeling.</p>